Dalton Transactions

Hexavacant γ-Dawson-type phosphotungstates supporting an edge-sharing bis(square-pyramidal) $\{O_2M(\mu_3\text{-}O)_2(\mu\text{-}OAc)MO_2\}$ core (M = Mn^{2+}, Co^{2+}, Ni^{2+}, Cu^{2+}, or Zn^{2+})

Journal:	*Dalton Transactions*
Manuscript ID	DT-ART-12-2018-004850.R2
Article Type:	Paper
Date Submitted by the Author:	09-Feb-2019
Complete List of Authors:	Suzuki, Kosuke; The University of Tokyo, Department of Applied Chemistry, School of Engineering, Minato, Takuo; The University of Tokyo, Department of Applied Chemistry, School of Engineering, Tominaga, Naoto; The University of Tokyo, Department of Applied Chemistry, School of Engineering, Okumo, Ichiro; The University of Tokyo, Department of Applied Chemistry, School of Engineering, Yonesato, Kentaro; The University of Tokyo, Department of Applied Chemistry, School of Engineering, Mizuno, Noritaka; The University of Tokyo, Department of Applied Chemistry Yamaguchi, Kazuya; The University of Tokyo, Department of Applied Chemistry

SCHOLARONE™
Manuscripts

Submitted to *Dalton Trans.* as a *Full Paper*

Hexavacant γ-Dawson-type phosphotungstates supporting an edge-sharing bis(square-pyramidal) $\{O_2M(\mu_3\text{-}O)_2(\mu\text{-}OAc)MO_2\}$ core (M = Mn^{2+}, Co^{2+}, Ni^{2+}, Cu^{2+}, or Zn^{2+})†

Kosuke Suzuki,* [a,b] Takuo Minato,[a] Naoto Tominaga,[a] Ichiro Okumo,[a] Kentaro Yonesato,[a] Noritaka Mizuno[a] and Kazuya Yamaguchi* [a]

[a]*Department of Applied Chemistry, School of Engineering, The University of Tokyo, 7-3-1 Hongo, Bunkyo-ku, Tokyo 113-8656, Japan. E-mail: ksuzuki@appchem.t.u-tokyo.ac.jp, kyama@appchem.t.u-tokyo.ac.jp*

[b]*Precursory Research for Embryonic Science and Technology (PRESTO), Japan Science and Technology Agency (JST), 4-1-8 Honcho, Kawaguchi, Saitama 332-0012, Japan*

†Electronic supplementary information (ESI) available: Experimental details, including IR and UV-vis spectra, magnetic data, CSI mass, NMR, CV. CCDC 1883422–1883426. For ESI and crystallographic data in CIF or other electronic format.

Abstract

In aqueous media, introduction of additional metal species into polyoxometalates (POMs) with multiple vacant sites, such as a hexavacant Dawson-type phosphotungstate, which is of interest for the synthesis of novel metal oxide clusters, is generally difficult because they easily undergo self-condensation and/or structural decomposition. In this study, we succeeded in developing a novel synthetic method to obtain metal-substituted γ-Dawson-type phosphotungstate monomers by introducing metal species into an organic solvent-soluble lacunary phosphotungstate $TBA_4H_{10}[\alpha\text{-}P_2W_{12}O_{48}]$ (**I**) (TBA = tetra-*n*-butylammonium) in organic media. The reaction of **I**, which possessed two types of vacant sites, i.e., middle and edge sites, with divalent metal species such as Mn^{2+}, Co^{2+}, Ni^{2+}, Cu^{2+}, or Zn^{2+} in acetonitrile afforded a series of isostructural POMs **M2** ($TBA_5[\gamma\text{-}P_2W_{12}O_{44}M_2(OAc)(CH_3CONH)_2]\cdot nH_2O\cdot mCH_3CN$; M = Mn^{2+}, Co^{2+}, Ni^{2+}, Cu^{2+}, or Zn^{2+}; OAc = acetate) with an edge-sharing bis(square-pyramidal) $\{O_2M(\mu_3\text{-}O)_2(\mu\text{-}OAc)MO_2\}$ core. The bis(square-pyramidal) core was selectively placed at the middle site of the hexavacant lacunary phosphotungstate, and the two metals in the core were bridged with two phosphate units and one acetate species. Meanwhile, the edge sites were capped by acetimidate ligands, which protect the reactive lacunary POM from self-condensation. To the best of our knowledge, this is the first report describing the synthesis and characterization of metal-substituted hexavacant γ-Dawson-type POM monomers.

Introduction

Polyoxometalates (POMs) are a unique class of discrete anionic metal oxide nanoclusters that exhibit large diversity in their structures.[1] Their physicochemical properties can be finely controlled by selecting structures, constituent elements, charges, and/or introducing metal cations, which provides access to potential applications in various fields including catalysis, photocatalysis, magnetism, electrochemistry, biomedicine, and materials science.[1] In particular, lacunary POMs, which lack some of the $\{M_xO_y\}$ units from the parent frameworks, act as structurally well-defined multidentate inorganic ligands for the synthesis of multinuclear metal oxide clusters exhibiting novel catalytic, redox, and magnetic properties.[2] Since the

structures and properties of the metal oxide clusters are associated with those of the lacunary POMs, the development of new lacunary POM units is highly desirable to achieve novel materials.

A hexavacant lacunary Dawson-type phosphotungstate ($[\alpha\text{-}P_2W_{12}O_{48}]^{14-}$, Fig. 1a) is a unique multidentate ligand that lacks a $\{W_6O_{14}\}$ unit from the parent Dawson-type framework ($[\alpha\text{-}P_2W_{18}O_{62}]^{6-}$);[3] it possesses large number of coordination sites than other lacunary structures, such as mono- and trivacant lacunary Dawson-type POMs (e.g., $[\alpha_2\text{-}P_2W_{17}O_{61}]^{10-}$ and $[\alpha\text{-}P_2W_{15}O_{56}]^{12-}$, Fig. 1b, c), and mono-, di-, and trivacant lacunary Keggin-type POMs (e.g., $[\alpha\text{-}XM_{11}O_{39}]^{n-}$, $[\gamma\text{-}XM_{10}O_{36}]^{n-}$, and $[\alpha\text{-}XM_9O_{34}]^{n-}$, Fig. 1d–f). In addition, it provides two types of vacant sites, whereas other lacunary POMs typically possess only one type of vacant sites (Fig. 1). These features provide the hexavacant lacunary phosphotungstate with great potential as a multidentate ligand for the synthesis of metal oxide clusters with unique structures and properties.[4-9] However, this species is metastable in aqueous media, which frequently results in decomposition of the structure. Moreover, controlling the reactivity of the large vacant sites is difficult. To date, only two crystallographic structures on the metal-substituted hexavacant α-Dawson-type POM monomers have been reported, where the vacant sites were fully occupied by metal atoms (Nb or Fe) upon the reaction of $[\alpha\text{-}P_2W_{12}O_{48}]^{14-}$ with the corresponding metal cations in aqueous media.[4] In addition, Mo and V have been introduced into the hexavacant α-Dawson-type POM monomers, albeit their structures have been studied only by spectroscopic analyses.[5] In other cases, $[\alpha\text{-}P_2W_{12}O_{48}]^{14-}$ has been shown to easily undergo decomposition[6,7] and/or condensation at the highly reactive vacant sites into dimer, trimer, or tetramer structures[8,9] during the reaction with metal cations in aqueous media. Consequently, control and estimation of the products are usually quite difficult. For example, upon reaction with $Fe(NO_3)_3$ and KOH in aqueous media, $[\alpha\text{-}P_2W_{12}O_{48}]^{14-}$ was transformed to $[P_2W_{14}O_{54}]^{14-}$ through incorporation of Fe^{3+}, affording a dimer $[H_{12}P_4W_{48}Fe_8O_{120}]^{16-}$.[7] Meanwhile, Fang, Kögerler, and coworkers reported the formation of a giant structure of formula $[Mn_{40}P_{32}W_{224}O_{888}]^{144-}$ through the complex reaction of $[\alpha\text{-}P_2W_{12}O_{48}]^{14-}$ and Mn^{3+} cations.[8]

To achieve inorganic materials with controlled structures and properties, we have engaged in developing a new synthetic method for metal oxide clusters in organic media by utilizing organic solvent-soluble tetra-*n*-butyl ammonium (TBA) salts of lacunary POMs, such as divacant and trivacant lacunary Keggin-type POMs.[10] In organic media, undesired decomposition of lacunary templates can be suppressed, thereby

allowing the precise synthesis of metal oxide clusters for investigating their unique catalytic, photocatalytic, and magnetic properties.[10] For example, we successfully synthesized heterometallic clusters by introducing several different metal species in a stepwise manner into lacunary POMs in organic media.[11] In addition, the synthesis of POMs in organic media enabled us to utilize organic protecting ligands such as alkoxides and acetimidate for the highly reactive vacant sites of lacunary POMs.[12]

Recently, we have reported the synthesis of an organic solvent-soluble TBA salt of a hexavacant lacunary Dawson-type POM ($[P_2W_{12}O_{48}]^{14-}$), which was successfully utilized for the construction of giant hexameric and tetrameric ring-shaped structures by the reaction with Mn^{3+} in dichloromethane (Fig. 2, route B).[13] Herein, we report the successful synthesis of metal-substituted γ-Dawson-type phosphotungstate monomers by introducing metal cations into a TBA salt of α-Dawson-type POM (**I**, $TBA_4H_{10}[\alpha\text{-}P_2W_{12}O_{48}]\cdot 6H_2O$) in acetonitrile (Fig. 2, route A). The reaction of **I** and divalent metal species such as Mn^{2+}, Co^{2+}, Ni^{2+}, Cu^{2+}, or Zn^{2+} in acetonitrile afforded a series of isostructural POMs **M2** ($TBA_5[\gamma\text{-}P_2W_{12}O_{44}M_2(OAc)(CH_3CONH)_2]\cdot nH_2O\cdot mCH_3CN$; M = Mn^{2+}, Co^{2+}, Ni^{2+}, Cu^{2+}, or Zn^{2+}; OAc = acetate) with an edge-sharing bis(square-pyramidal) $\{O_2M(\mu_3\text{-}O)_2(\mu\text{-}OAc)MO_2\}$ core (Fig. 3). Notably, the α-Dawson-type structure was transformed into a γ-Dawson type structure by introducing the dinuclear metal core on the middle vacant site.

Results and discussion

The TBA salt of a hexavacant lacunary α-Dawson-type POM (**I**) was synthesized by the reaction of $K_{12}H_2[\alpha\text{-}P_2W_{12}O_{48}]\cdot 24H_2O$[3] with TBABr in aqueous nitric acid according to our previous procedure.[13] The IR spectrum of **I** showed three bands assignable to the stretching vibrations of P–O bonds of the $\{PO_4\}$ units at 1145, 1086, and 1025 cm^{-1} similar to those of the starting $K_{12}H_2[\alpha\text{-}P_2W_{12}O_{48}]\cdot 24H_2O$ (1130, 1075, and 1012 cm^{-1}), indicating that **I** possessed a hexavacant lacunary α-Dawson-type structure (Fig. 4a, b). The molecular formula of **I** was established to be $TBA_4H_{10}[\alpha\text{-}P_2W_{12}O_{48}]\cdot 6H_2O$ by elemental analysis.

The synthesis of **Mn2** was carried out by reacting **I** with $Mn(OAc)_2$ in 1:2 molar ratio in acetonitrile. The acetonitrile solution containing **I** and $Mn(OAc)_2$ was stirred for 3 h at 60 °C. Then, tetra-*n*-

butylammonium hydroxide (TBAOH, 1 equivalent with respect to **I**) was added, and the solution was stirred for additional 12 h at 60 °C. The positive-ion cold spray ionization (CSI)-mass spectrum of the reaction solution showed only a major set of signals at *m/z* 4711.6, which can be assigned to $[TBA_6P_2W_{12}O_{44}Mn_2(OAc)(CH_3CONH)_2]^+$ (Fig. S1a, ESI†). By pouring the solution into diethyl ether, a brown precipitate of **Mn2** was obtained in 95% yield (based on **I**). In contrast, when the reaction of **I** and $Mn(OAc)_2$ was carried out in other organic solvents such as acetone, 1,2-dichloroethane, and dichloromethane, positive-ion CSI-mass analysis revealed the formation of a complex mixture; thus, in dichloromethane, sets of signals at *m/z* 4542.6, 4700.6, 4881.8, 8842.1, 9156.5, and 9441.5 assignable to dimers of $[P_2W_{12}O_{48}]^{14-}$ incorporating several Mn^{2+} cations were observed (Fig. S1b, ESI†). We have recently reported that the reaction of **I** with $Mn(acac)_3$ (acac = acetylacetonato) in 1:4 molar ratio in dichloromethane gave giant hexamers and tetramers of Mn-substituted hexavacant lacunary γ-Dawson-type POM units.[13] These results indicated that the use of acetonitrile was crucial to obtain the monomer structure.

Single crystals suitable for X-ray crystallographic analysis were successfully obtained by recrystallization of the powder sample of **Mn2** from a mixture of acetonitrile and diethyl ether. The crystallographic analysis revealed that a dinuclear Mn core was formed selectively on the middle site of the hexavacant lacunary Dawson-type structure (Table 1, Fig. 3, S2, ESI†). Two Mn atoms were bridged by two oxygen atoms of both $\{PO_4\}$ units and one acetate ligand. The other two vacant sites (edge sites) were capped by two acetimidate ligands (CH_3CONH), which were possibly formed by the hydration of acetonitrile.[14] These results agreed with the solvent effects observed on the synthesis, confirming that the use of acetonitrile as the synthetic solvent is crucial because the hydrated products, i.e., acetimidate ligands, act as protecting ligands to inhibit undesired oligomerization reactions at the highly reactive vacant sites. Notably, the framework of Dawson-type POM was transformed from α to γ-type by flipping the $\{PO_4\}$ units upon incorporation of the Mn^{2+} cations (Fig. 5). This was supported by the stretching vibrations of P–O bonds of the $\{PO_4\}$ units of **Mn2** (1066 and 1037 cm^{-1}), which differ significantly from those of **I** and $K_{12}H_2[\alpha\text{-}P_2W_{12}O_{48}]\cdot 24H_2O$ (Fig. 4). Although the reactions of hexavacant lacunary Dawson-type POMs with metal cations in aqueous media have been examined by several groups, to the best of our knowledge, no

report has been published on the formation of a metal-substituted hexavacant lacunary γ-Dawson-type POM monomer.[4–9]

The anion of **Mn2** possessed a unique edge-sharing bis(square-pyramidal) $\{O_2Mn(\mu_3\text{-}O)_2(\mu\text{-}OAc)MnO_2\}$ core on the vacant site of the γ-Dawson-type POM. The coordination geometry of each Mn atom was close to a five-coordinate square pyramid; each Mn atom was coordinated by two oxygen atoms from both $\{PO_4\}$ units, two oxygen atoms of the vacant site of the POM framework, and one oxygen atom of the acetate ligand (CH_3COO). To the best of our knowledge, only a few reports on edge-sharing square-pyramidal Mn^{2+} cores where the axial ligands of two Mn^{2+} point toward the same direction have been reported.[15] The bond valence sum (BVS) values for Mn (2.11), P (4.81), and W (5.97–6.45) indicated that the respective valences were +2, +5, and +6 (Table S1, ESI†). In addition, the BVS values of the oxygen atoms were in the range 1.60–2.19 (Table S1, ESI†), thus, indicating the absence of protons on the oxygen atoms of the anion. Finally, the Mn–O–Mn bridging angles and Mn···Mn distance were 88.3° and 3.047 Å, respectively (Table 2).

The positive-ion CSI-mass spectrum of the crystals recorded in acetonitrile showed a set of signals at *m/z* 4711.8 assignable to $[TBA_6P_2W_{12}O_{44}Mn_2(OAc)(CH_3CONH)_2]^+$ (Fig. 6), which is indicative of the stability of **Mn2** in this solution. Meanwhile, the UV–vis absorption spectrum of **Mn2** in acetonitrile exhibited a band at 280 nm (3.57×10^2 M^{-1} cm^{-1}) that can be attributed to the O-to-W^{6+} charge transfer (Fig. S3a, ESI†). The oxidation state of Mn^{2+} was supported by the direct current (dc) magnetic susceptibility measurement of the polycrystalline sample of **Mn2** under 0.1 T, which showed that the χT value at 300 K (7.79 cm^3 K mol^{-1}) was close to the spin-only value for two Mn^{2+} (8.75 cm^3 K mol^{-1}; $S = 5/2$, $g = 2.00$) (Fig. 7). Elemental analysis showed the existence of five TBA cations per anion and the Mn:P:W ratio of 2:2:12 in accord with the CSI-mass data. On the basis of these results and that of a TG analysis, the formula of **Mn2** can be expressed as $TBA_5[\gamma\text{-}P_2W_{12}O_{44}Mn_2(OAc)(CH_3CONH)_2]\cdot 7H_2O\cdot CH_3CN$.

Following a similar procedure, other dinuclear structures **M2** (M = Co, Ni, Cu, and Zn) were also synthesized by the reaction of **I** with $M(OAc)_2$ in 1:2 molar ratio in acetonitrile. The crystal structures of **Co2**, **Ni2**, **Cu2**, and **Zn2** could be successfully determined by X-ray crystallographic analysis. Their anion structures were intrinsically isostructural with that of **Mn2** (Table 1, Fig. 3, S2, ESI†). Dinuclear cores

possessing five-coordinate square pyramidal coordination geometries were observed on the middle sites of the hexavacant lacunary Dawson-type structures. Notably, all these compounds possessed γ-Dawson-type structures. Two oxygen atoms from both $\{PO_4\}$ units and one acetate ligand bridged the M^{2+} cations. The BVS values for Co (1.96), Ni (1.95), Cu (2.11), and Zn (2.05) indicated that the valances of all these metals were +2 (Table S1, ESI†). The M···M distances were 3.047 (**Mn2**), 2.985 (**Co2**), 2.893 (**Ni2**), 2.892 (**Cu2**), and 2.956 (**Zn2**) (Table 2). Since the rigid γ-Dawson-type POM framework provided unique rectangular-shaped coordination sites consisting of six oxygen atoms (O1, O2, O3, O1*, O2*, O3*) at the vacant sites, the M–O–M bridging angles of dinuclear cores became close to 90°. The M–O–M bridging angles of the dinuclear cores increased in the following order: 88.3° (**Mn2**) < 88.7° (**Zn2**) < 89.6° (**Co2**) < 89.8° (**Ni2**) < 90.9° (**Cu2**) (Table 2), which can be roughly correlated with the order of the ionic radii of the corresponding M^{2+} ions (high spin, five-coordinate): 0.75 Å (Mn^{2+}) > 0.68 Å (Zn^{2+}) > 0.67 Å (Co^{2+}) > 0.65 Å (Cu^{2+}) > 0.63 Å (Ni^{2+}); i.e., the M–O–M bridging angles increased when decreasing the ionic radii of the cations. Divalent transition metal cations ($M(OAc)_2$) was used to synthesize all these structures. In contrast, when we used trivalent transition metal cations such as $Mn(OAc)_3$, $Fe(acac)_3$, and $Co(OAc)_3$, dinuclear structures could not be obtained. Nevertheless, $Mn(acac)_3$ was also effective for the synthesis of **Mn2**, due presumably to the reduction of Mn^{3+} to Mn^{2+} that takes place through the oxidative C–C bond cleavage of acetylacetone during the reaction of $Mn(acac)_3$ with the hexavacant lacunary POM.[13,16]

The positive-ion CSI-mass spectra of the crystals of **M2** in acetonitrile showed sets of signals at *m/z* 4720.2 (**Co2**), 4720.0 (**Ni2**), 4729.5 (**Cu2**), and 4733.5 (**Zn2**) assignable to $[TBA_6P_2W_{12}O_{44}M_2(OAc)(CH_3CONH)_2]^+$ (Fig. S4, ESI†). In addition, the ^{31}P NMR spectrum of **Zn2** recorded in dichloromethane-d_2 exhibited a single signal at 0.36 ppm (Fig. S5, ESI†), together with the mass spectra results, indicating that **M2** were stable and existed as single species in these solvents. The cyclic voltammograms of **M2** showed the W^{6+}/W^{5+} redox waves in the range of –2 to –1 V (Fig. S6, ESI†). The W^{6+}/W^{5+} redox waves for **Cu2** and **Zn2** were observed in the different redox potential from those of **Mn2**, **Co2**, and **Ni2**. One of the possible reasons for the differences in the cyclic voltammograms is that reduction of the substituted metals proceeded in these compounds. The UV–vis absorption spectra of **M2** showed bands attributable to the O-to-W^{6+} transition (ca. 280 nm) and the d–d transitions of M^{2+} cations except for

Zn2 (Fig. S3, ESI†): 499 nm (1.40×10^2 M^{-1} cm^{-1}), 591 nm (1.40×10^2 M^{-1} cm^{-1}), and 627 nm (1.30×10^2 M^{-1} cm^{-1}) for **Co2**; 494 nm (1.29×10^2 M^{-1} cm^{-1}) and 835 nm (3.13×10 M^{-1} cm^{-1}) for **Ni2**; and 905 nm (9.21×10 M^{-1} cm^{-1}) for **Cu2**.

Taking these results together with the elemental and TG analyses, the molecular formulas of these compounds were determined to be $TBA_5[\gamma\text{-}P_2W_{12}O_{44}M_2(OAc)(CH_3CONH)_2]\cdot nH_2O\cdot mCH_3CN$ (**Co2**, M = Co, n = 7, m = 0; **Ni2**, M = Ni, n = 6, m = 1; **Cu2**, M = Cu, n = 8, m = 1; **Zn2**, M = Zn, n = 8, m = 1). Taking into account the transformation of the α-type structures to the unique γ-type structures that occurred during the introduction of the metal cations, the formation of **M2** can be expressed by the following equation:

$$TBA_4H_{10}[\alpha\text{-}P_2W_{12}O_{48}] + 2M(OAc)_2 + TBAOH + 2CH_3CN$$

$$\rightarrow TBA_5[\gamma\text{-}P_2W_{12}O_{44}M_2(OAc)(CH_3CONH)_2] + 3AcOH + 3H_2O$$

The dc magnetic susceptibilities of polycrystalline samples of the paramagnetic derivatives **Mn2**, **Co2**, **Ni2**, and **Cu2** were measured under a dc magnetic field of 0.1 T in a temperature range of 1.9–300 K (Fig. 7). We found that the χT value of **Mn2** continuously decreased with decreasing temperature from 300 K to 1.9 K, indicating the presence of predominant antiferromagnetic interactions between Mn^{2+} ions. In contrast, the χT values of **Co2** and **Cu2** increased with decreasing temperature, which is consistent with the occurrence of ferromagnetic interactions between M^{2+} cations (M^{2+} = Co^{2+} or Cu^{2+}). In the case of **Ni2**, the χT value increased with decreasing temperature in the range of ca. 20–150 K, followed by a sharp decrease of the χT value below ca. 25 K. The increase of the χT value is most likely due to the ferromagnetic interactions between Ni^{2+} cations, while the decrease of the χT value at low temperature (<ca. 20 K) can be partially attributed to the contribution of orbital angular momentum. The intramolecular magnetic interactions J between M^{2+} cations were estimated by using the PHI program to be –4.82 cm^{-1} for **Mn2**, 3.01 cm^{-1} for **Ni2**, and 19.6 cm^{-1} for **Cu2**.[17,18]

Conclusions

In conclusion, we report a novel synthetic method for metal-substituted γ-Dawson-type POM monomers of formula $TBA_5[\gamma\text{-}P_2W_{12}O_{44}M_2(OAc)(CH_3CONH)_2]\cdot nH_2O\cdot mCH_3CN$ (**M2**, M = Mn^{2+}, Co^{2+}, Ni^{2+}, Cu^{2+}, or Zn^{2+}) that consists of the reaction of a TBA salt of an α-Dawson-type POM (**I**, $TBA_4H_{10}[\alpha\text{-}P_2W_{12}O_{48}]$) with metal species in organic media. The unique edge-sharing bis(square-pyramidal) $\{O_2M(\mu_3\text{-}O)_2(\mu\text{-}OAc)MO_2\}$ core is incorporated on the middle site of the obtained hexavacant lacunary γ-Dawson-type POM, and two acetimidate ligands act as protecting groups for the highly reactive vacant sites. Since these acetimidate ligands are most likely easily removable by hydrolysis, the **M2** series can be envisaged as a new family of lacunary POM precursors for the synthesis of multinuclear and/or heterometallic structures.

Experimental

Materials

Acetonitrile (Kanto Chemical), dichloromethane (Kanto Chemical), diethyl ether (Kanto Chemical), nitric acid (Kanto Chemical), tetra-*n*-butylammonium bromide (TCI), tetra-*n*-butylammonium hydroxide solution in methanol (Aldrich), $Mn(OAc)_2\cdot 4H_2O$ (Kanto Chemical), $Mn(acac)_3$ (Aldrich), $Co(OAc)_2$ (Aldrich), $Ni(OAc)_2\cdot 4H_2O$ (Kanto Chemical), $Cu(OAc)_2$ (Kanto Chemical), $Zn(OAc)_2\cdot 2H_2O$ (Kanto Chemical) were used as received. $K_{12}H_2[\alpha\text{-}P_2W_{12}O_{48}]\cdot 24H_2O$ was synthesized according to the reported procedure.[3]

Instruments

IR spectra were measured on JASCO FT/IR-4100 using KBr disks. UV-vis spectra were measured on JASCO V-570. CSI-mass spectra were recorded on JEOL JMS-T100CS. NMR spectra were recorded on JEOL JMN ECA-500 spectrometer (^{1}H, 500.16 MHz; ^{31}P, 202.47 MHz) by using 5 mm tubes. Chemical shifts (δ) were reported in ppm downfield from $SiMe_4$ (solvent, $CDCl_3$) for ^{1}H NMR spectra and upfield from H_3PO_4 (solvent, D_2O) for ^{31}P NMR spectra. Thermogravimetric and differential thermal analyses (TG-DTA) were performed on Rigaku Thermo plus TG 8120. ICP-AES analyses for Mn, Co, Ni, Cu, Zn, P, and W were performed with Shimadzu ICPS-8100. Elemental analyses were performed on Elementar vario

MICRO cube (for C, H, and N) at the Elemental Analysis Center of School of Science of the University of Tokyo.

X-ray crystallography

Diffraction measurements were made on a Rigaku MicroMax-007 Saturn 724 CCD detector with graphic monochromated Mo Kα radiation (λ = 0.71069 Å, 50 kV, 24 mA) at 123 K. The data were collected and processed using CrystalClear[19] and HKL2000.[20] Neutral scattering factors were obtained from the standard source. In the reduction of data, Lorentz and polarization corrections were made. The structural analyses were performed using CrystalStructure[21] and WinGX.[22] All structures were solved by SHELXS-97 (direct methods) and refined by SHELXL-2014.[23] The metal atoms (W, Mn, Co, Ni, Cu, and Zn), P, and O atoms in the POM frameworks were refined anisotropically. CCDC-1883422 (**Mn2**), -1883423 (**Co2**), -1883424 (**Ni2**), -1883425 (**Cu2**), and -1883426 (**Zn2**) contain the supplementary crystallographic data for this paper. The data can be obtained free of charge via www.ccdc.cam.ac.uk/conts/retrieving.html (or from the Cambridge Crystallographic Data Centre, 12, Union Road, Cambridge CB2 1EZ, UK; Fax: (+44) 1223-336-033; or deposit@ccdc.cam.ac.uk).

Bond valence sum (BVS) calculations

The BVS values were calculated by the expression for the variation of the length r_{ij} of a bond between two atoms i and j in observed crystal with valence V_i.

$$V_i = \sum_j \exp\left(\frac{r_0' - r_{ij}}{B}\right)$$

where B is constant equal to 0.37 Å, r'_0 is bond valence parameter for a given atom pair.[24]

Magnetic susceptibilities

Magnetic susceptibilities of polycrystalline samples were measured on Quantum Design MPMS-XL7. Direct current (dc) magnetic susceptibility measurements were carried out between 1.9 and 300 K under 0.1 T magnetic field. Diamagnetic corrections were applied by the diamagnetisms of the sample holder and $TBA_4H_{10}[P_2W_{12}O_{48}]\cdot 6H_2O$. Spin Hamiltonian can be expressed by the following equation: $\boldsymbol{H} = \boldsymbol{H}_{\mathbf{SO}} + \boldsymbol{H}_{\mathbf{EX}} + \boldsymbol{H}_{\mathbf{ZEE}}$ ($\boldsymbol{H}_{\mathbf{SO}}$, spin orbit coupling; $\boldsymbol{H}_{\mathbf{EX}}$, exchange coupling; $\boldsymbol{H}_{\mathbf{ZEE}}$, Zeeman effect). The magnetic interactions

were analyzed by fitting the temperature-dependence of magnetic susceptibilities using the PHI program (*J*, exchange constant of M^{2+}–M^{2+} ; *D*, zero-field splitting parameter (for **Ni2**, $D = 19.6\ cm^{-1}$)).[17]

Electrochemistry

Cyclic voltammetric measurements were carried out with Solartron SI 1287 Electrochemical Interface. A standard three-electrode arrangement was employed with a BAS glassy carbon disk electrode as the working electrode, a platinum wire as the counter electrode, and a silver wire electrode as the pseudoreference electrode. The voltage scan rate was set at 100 mV s^{-1}, and $TBAClO_4$ was used as an electrolyte.

Synthesis and characterization of $TBA_4H_{10}[\alpha\text{-}P_2W_{12}O_{48}]\cdot 6H_2O$ (I)

$TBA_4H_{10}[\alpha\text{-}P_2W_{12}O_{48}]\cdot 6H_2O$ (**I**) was synthesized according to our recent procedure.[13] $K_{12}H_2[\alpha\text{-}P_2W_{12}O_{48}]\cdot 24H_2O$ (8.59 g, 2.18 mmol) was dissolved in nitric acid solution (287 mL, containing 8 equivalents of HNO_3 with respect to $K_{12}H_2[\alpha\text{-}P_2W_{12}O_{48}]\cdot 24H_2O$), and TBABr (56.9 g, 176 mmol) was added. After vigorous stirring for 1 min, white precipitate formed was isolated by filtration and washed with water (4 °C, 84 mL) for 3 min, followed by drying in vacuo for 24 h (7.63 g, 86% yield). IR (KBr pellet): 3420, 2961, 2873, 1653, 1635, 1559, 1485, 1382, 1348, 1145, 1086, 1025, 946, 927, 887, 816, 737, 543, 460, 372, 351, 318, 304, 296, 282, 267, 253 cm^{-1}. ^{31}P NMR (202.47 MHz, the mixed solvent of acetone-d_6 and methanol (1:1, v/v), 298 K, H_3PO_4) δ = –7.6 ppm. Elemental analysis calcd. (%) for $TBA_4H_{10}[\alpha\text{-}P_2W_{12}O_{48}]\cdot 6H_2O$ ($C_{64}H_{166}N_4O_{54}P_2W_{12}$): C 18.64, H 4.06, N 1.36, P 1.50, W 53.49; found, C 18.95, H 3.96, N 1.43, P 1.41, W 52.46.

Synthesis and characterization of $TBA_5[\gamma\text{-}P_2W_{12}O_{44}Mn_2(OAc)(CH_3CONH)_2]\cdot 7H_2O\cdot CH_3CN$ (Mn2)

$Mn(OAc)_2$ (77 mg, 0.44 mmol) was dissolved in acetonitrile (30 mL), and **I** (900 mg, 0.22 mmol) was added to the solution at room temperature. After stirring the solution for 3 h at 60 °C, TBAOH (1 equivalent with respect to **I**) was added. After stirring the solution for additional 12 h at 60 °C, the reaction solution was poured into diethyl ether (1.2 L). Brown precipitate (**Mn2**) formed was isolated by filtration, followed by drying in vacuo for 24 h (952 mg, 94% yield). By recrystallization of **Mn2** in a mixture of acetonitrile and diethyl ether at 45 °C, brown plate single crystals were obtained (27 % yield for recrystallization). **Mn2** could be also synthesized by the reaction of $Mn(acac)_3$ and **I**: $Mn(acac)_3$ (154 mg, 0.44 mmol) was dissolved in acetonitrile (30 mL), and **I** (900 mg, 0.22 mmol) was added. After stirring for 1 h at 60 °C, TBAOH (1

equivalent with respect to **I**) was added. After stirring for 12 h at 60 °C, the reaction solution was poured into diethyl ether (1.2 L). Brown precipitate (**Mn2**) formed was isolated by filtration, followed by drying in vacuo for 24 h (865 mg, 95% yield). By recrystallization of **Mn2** (320 mg) in a mixture of acetonitrile and diethyl ether at 45 °C, brown plate single crystals for X-ray crystallographic analysis, elemental analysis, and spectroscopic analysis were obtained (50.5 mg, 16 % yield for recrystallization). IR (KBr pellet): 3421, 2961, 2931, 2874, 2737, 1663, 1573, 1484, 1466, 1379, 1349, 1280, 1253, 1216, 1150, 1066, 1037, 941, 872, 810, 565, 531, 458, 409, 393, 360, 325, 299, 279, 265, 257, 253 cm^{-1}. UV-vis (acetonitrile): λ (ε) 275 nm (3.02×10^4 M^{-1} cm^{-1}). Positive ion MS (CSI, acetonitrile): *m/z* 4711.8 (calcd. 4711.8) $[TBA_6P_2W_{12}O_{44}Mn_2(OAc)(CH_3CONH)_2]^+$. Elemental analysis calcd. (%) for $TBA_5P_2W_{12}O_{44}Mn_2(OAc)(CH_3CONH)_2 \cdot 7H_2O \cdot CH_3CN$ ($C_{88}H_{208}N_8O_{55}P_2W_{12}Mn_2$), C 22.79, H 4.49, N 2.42, P 1.34, W 47.58, Mn 2.37.; found, C 22.79, H 4.50, N 2.49, P 1.39, W 49.75, Mn 2.38.

Synthesis and characterization of $TBA_5[\gamma\text{-}P_2W_{12}O_{44}Co_2(OAc)(CH_3CONH)_2] \cdot 7H_2O$ (Co2)

$Co(OAc)_2$ (77 mg, 0.44 mmol) was dissolved in acetonitrile (30 mL), and **I** (900 mg, 0.22 mmol) was added to the solution at room temperature. After stirring the solution for 3 h at 60 °C, TBAOH (1 equivalent with respect to **I**) was added. After stirring the solution for additional 12 h at 60 °C, the reaction solution was poured into diethyl ether (1.2 L). Dark blue precipitate (**Co2**) formed was isolated by filtration, followed by drying in vacuo for 24 h (967 mg, 95% yield). By recrystallization of **Co2** (320 mg) in a mixture of acetonitrile and diethyl ether at 45 °C, dark blue plate single crystals for X-ray crystallographic analysis, elemental analysis, and spectroscopic analysis were obtained (83.5 mg, 26 % yield for recrystallization). IR (KBr pellet): 3420, 2962, 2935, 2874, 1663, 1576, 1485, 1433, 1382, 1346, 1283, 1247, 1069, 1035, 943, 817, 722, 580, 562, 529, 464, 498, 360, 356, 317, 311, 296, 283 cm^{-1}. UV-vis (acetonitrile): λ (ε) 280 nm (3.57×10^4 M^{-1} cm^{-1}), 499 nm (1.40×10^2 M^{-1} cm^{-1}), 591 nm (1.40×10^2 M^{-1} cm^{-1}), 627 nm (1.30×10^2 M^{-1} cm^{-1}). Positive ion MS (CSI, acetonitrile): *m/z* 4720.2 (calcd. 4719.8) $[TBA_6P_2W_{12}O_{44}Co_2(OAc)(CH_3CONH)_2]^+$, 2481.3 (calcd. 2481.0) $[TBA_7P_2W_{12}O_{44}Co_2(OAc)(CH_3CONH)_2]^{2+}$. Elemental analysis calcd. (%) for $TBA_5P_2W_{12}O_{44}Co_2(OAc)(CH_3CONH)_2 \bullet 7H_2O$ ($C_{86}H_{205}N_7O_{55}P_2W_{12}Co_2$), C 22.44, H 4.48, N 2.13, P 1.35, W 47.92, Co 2.56.; found, C 22.33, H 4.48, N 2.10, P 1.34, W 47.97, Co 2.62.

Synthesis and characterization of $TBA_5[\gamma\text{-}P_2W_{12}O_{44}Ni_2(OAc)(CH_3CONH)_2] \cdot 6H_2O \cdot CH_3CN$ (Ni2)

$Ni(OAc)_2 \cdot 4H_2O$ (109 mg, 0.44 mmol) was dissolved in acetonitrile (30 mL), and **I** (900 mg, 0.22 mmol) was added to the solution at room temperature. After stirring the solution for 3 h at 60 °C, TBAOH (1 equivalent with respect to **I**) was added. After stirring the solution for additional 12 h at 60 °C, the reaction solution was poured into diethyl ether (1.0 L). Yellow precipitate (**Ni2**) formed was isolated by filtration, followed by drying in vacuo for 24 h (963 mg, 95% yield). By recrystallization of **Ni2** (320 mg) in a mixture of acetonitrile and diethyl ether at 45 °C, dark blue plate single crystals for X-ray crystallographic analysis, elemental analysis, and spectroscopic analysis were obtained (83.5 mg, 26 % yield for recrystallization). IR (KBr pellet): 3420, 3199, 2961, 2936, 2874,1663, 1577, 1545, 1486,1464, 1432, 1383, 1346, 1313, 1285, 1252, 1150, 1105, 1073, 1034, 943, 812, 722, 565, 459, 409, 361, 329, 299, 282, 275, 268, 254 cm^{-1}. UV-vis (acetonitrile): λ (ε) 279 nm (3.19×10^4 M^{-1} cm^{-1}), 494 nm (1.29×10^2 M^{-1} cm^{-1}), 835 nm (3.13×10 M^{-1} cm^{-1}). Positive ion MS (CSI, acetonitrile): *m/z* 4720.0 (calcd. 4719.4) $[TBA_6P_2W_{12}O_{44}Ni_2(OAc)(CH_3CONH)_2]^+$, 2481.3 (calcd. 2480.9) $[TBA_7P_2W_{12}O_{44}Ni_2(OAc)(CH_3CONH)_2]^{2+}$. Elemental analysis calcd. (%) for $TBA_5P_2W_{12}O_{44}Ni_2(OAc)(CH_3CONH)_2 \cdot 6H_2O \cdot CH_3CN$ ($C_{88}H_{206}N_8Ni_2O_{54}P_2W_{12}$), C 22.85, H 4.48, N 2.42, P 1.34, W 47.68, Ni 2.54.; found, C 22.62, H 4.42, N 2.43, P 1.34, W 49.50, Ni 2.53.

Synthesis and characterization of $TBA_5[\gamma\text{-}P_2W_{12}O_{44}Cu_2(OAc)(CH_3CONH)_2] \cdot 8H_2O \cdot CH_3CN$ (Cu2)

$Cu(OAc)_2$ (79 mg, 0.44 mmol) was dissolved in acetonitrile (30 mL), and **I** (900 mg, 0.22 mmol) was added to the solution at room temperature. After stirring the solution for 3 h at 60 °C, TBAOH (1 equivalent with respect to **I**) was added. After stirring the solution for additional 12 h at 60 °C, the reaction solution was poured into diethyl ether (1.0 L). Pale blue precipitate (**Cu2**) formed was isolated by filtration, followed by drying in vacuo for 24 h (945 mg, 94% yield). By recrystallization of **Cu2** (400 mg) in a mixture of acetonitrile and diethyl ether at 45 °C, light blue plate single crystals for X-ray crystallographic analysis, elemental analysis, and spectroscopic analysis were obtained (90.3 mg, 22 % yield for recrystallization). IR (KBr pellet): 3420, 3196, 2961, 2934, 2874,1662, 1577, 1486,1413, 1382, 1345, 1282, 1252, 1151, 1078, 1040, 1008, 945, 872, 806, 722, 580, 562, 518, 463, 411, 361, 354, 328, 318, 304, 298, 281 cm^{-1}. UV-vis (acetonitrile): λ (ε) 280 nm (2.86×10^4 M^{-1} cm^{-1}), 905 nm (9.21×10 M^{-1} cm^{-1}). Positive ion MS (CSI, acetonitrile): *m/z* 4729.5 (calcd. 4729.0) $[TBA_6P_2W_{12}O_{44}Cu_2(OAc)(CH_3CONH)_2]^+$, 2486.3 (calcd. 2485.8) $[TBA_7P_2W_{12}O_{44}Cu_2(OAc)(CH_3CONH)_2]^{2+}$. Elemental analysis calcd. (%) for

$TBA_5P_2W_{12}O_{44}Cu_2(OAc)(CH_3CONH)_2 \cdot 8H_2O \cdot CH_3CN$ ($C_{88}H_{210}N_8O_{56}P_2W_{12}Cu_2$), C 22.62, H 4.53, N 2.40, P 1.33, W 47.22, Cu 2.72.; found, C 22.24, H 4.43, N 2.39, P 1.32, W 47.65, Cu 2.72.

Synthesis and characterization of $TBA_5[\gamma\text{-}P_2W_{12}O_{44}Zn_2(OAc)(CH_3CONH)_2]\cdot 8H_2O\cdot CH_3CN$ (Zn2)

$Zn(OAc)_2\cdot 2H_2O$ (96 mg, 0.44 mmol) was dissolved in acetonitrile (30 mL), and **I** (900 mg, 0.22 mmol) was added to the solution at room temperature. After stirring the solution for 3 h at 60 °C, TBAOH (1 equivalent with respect to **I**) was added. After stirring the solution for additional 12 h at 60 °C, the reaction solution was poured into diethyl ether (1.0 L). Colorless precipitate (**Zn2**) formed was isolated by filtration, followed by drying in vacuo for 24 h (958 mg, 94% yield). By recrystallization of **Zn2** (300 mg) in a mixture of acetonitrile and diethyl ether at 45 °C, colorless plate single crystals for X-ray crystallographic analysis, elemental analysis, and spectroscopic analysis were obtained (46.2 mg, 15% yield for recrystallization). IR (KBr pellet): 3434, 3200, 2962, 2936, 2874,1665, 1582, 1544, 1486, 1461, 1436, 1382, 1345, 1311, 1285, 1254, 1151, 1071, 1029, 942, 881, 809, 721, 562, 456, 721, 562, 456, 408, 393, 360, 320, 300, 284, 270, 266, 260 cm^{-1}. UV-vis (acetonitrile): λ (ε) 273 nm (3.32×10^4 M^{-1} cm^{-1}). ^{31}P NMR (202.47 MHz, dichloromethane-d_2, 298 K, H_3PO_4) δ = 0.36 ppm. Positive ion MS (CSI, acetonitrile): *m/z* 4733.5 (calcd. 4732.8) $[TBA_6P_2W_{12}O_{44}Zn_2(OAc)(CH_3CONH)_2]^+$, 2488.5 (calcd. 2487.6) $[TBA_7P_2W_{12}O_{44}Zn_2(OAc)(CH_3CONH)_2]^{2+}$. Elemental analysis calcd. (%) for $TBA_5P_2W_{12}O_{44}Zn_2(OAc)(CH_3CONH)_2 \cdot 8H_2O \cdot CH_3CN$ ($C_{88}H_{210}N_8O_{56}P_2W_{12}Zn_2$), C 22.61, H 4.53, N 2.40, P 1.32, W 47.18, Zn 2.80.; found, C 22.58, H 4.51, N 2.36, P 1.33, W 47.57, Zn 2.90.

Acknowledgments

This work was supported in part by JSPS KAKENHI Grant Numbers 17H03037, JST PRESTO Grant Number JPMJPR18T7, and JST CREST Grant Number JPMJCR17P4. T. M. was supported by the JSPS through a Research Fellowship for Young Scientists.

Notes and references

(1) (*a*) M. T. Pope, *Heteropoly and Isopoly Oxometalates*, Springer, Berlin, 1983; (*b*) N. Mizuno and M. Misono, *Chem. Rev.*, 1998, **98**, 19; (*c*) M. Sadakane and E. Steckhan, *Chem. Rev.*, 1998, **98**, 219; (*d*) C. L. Hill, in *Comprehensive Coordination Chemistry II* (Eds.: J. A. McCleverty, T. J. Meyer), Elsevier Pergamon, Amsterdam, 2004, vol. 4, pp. 679; (*e*) U. Kortz, A. Müller, A.; J. Van Slageren, J. Schnack, N.S. Dalal and M. Dressel, *Coord. Chem. Rev.*, 2009, **253**, 2315; (*f*) D.-L. Long, R. Tsunashima and L. Cronin, *Angew. Chem., Int. Ed.*, 2010, **49**, 1736; (*g*) C. Streb, *Dalton Trans.*, 2012, **41**, 1651; (*h*) R. Eldik and L. Cronin, Eds. *Advances in Inorganic Chemistry*, Elsevier Academic Press, Amsterdam, 2017, vol. 69; (*i*) K. Suzuki, N. Mizuno and K. Yamaguchi, *ACS Catal.*, 2018, **8**, 10809.

(2) (*a*) P. Putaj and F. Lefebvre, *Coord. Chem. Rev.*, 2011, **255**, 1642; (*b*) O. Oms, A. Dolbecq and P. Mialane, *Chem. Soc. Rev.*, 2012, **41**, 7497; (*c*) S.-T. Zheng and G.-Y. Yang, *Chem. Soc. Rev.,* 2012, **41**, 7623.

(3) (*a*) R. Contant, *Inorg. Synth.*, 1990, **27**, 104; (*b*) R. Contant and J. P. Ciabrini, *J. Chem. Res., Synop.*, 1977, 222; *J. Chem. Res., Miniprint*, 1977, 2601.

(4) (*a*) D. A. Judd, Q. Chen, C. F. Campana and C. L. Hill, *J. Am. Chem. Soc.*, 1997, **119**, 5461; (*b*) B. Godin, Y.-G. Chen, J. Vaissermann, L. Ruhlmann, M. Verdaguer and P. Gouzerh, *Angew. Chem., Int. Ed.*, 2005, **44**, 3072.

(5) R. Contant, M. Abbessi, R. Thouvenot and G. Hervé, *Inorg. Chem.* 2004, **43**, 3597.

(6) Y.-W. Li, Y.-G. Li, Y.-H. Wang, X.-J. Feng, Y. Luv and E.-B. Wang, *Inorg. Chem.*, 2009, **48**, 6452.

(7) B. Godin, J. Vaissermann, P. Herson, L. Ruhlmann, M. Verdaguer and P. Gouzerh, *Chem. Commun.*, 2005, 5624.

(8) X. Fang, P. Kögerler, Y. Furukawa, M. Speldrich and M. Luban, *Angew. Chem., Int. Ed.* 2011, **50**, 5212.

(9) Z. Zhang, S. Yao, Y.- F. Qi, Y. Li, Y. Wang and E.- B. Wang, *Dalton Trans.*, 2008, 3051.

(10) (*a*) K. Suzuki, Y. Kikukawa, S. Uchida, H. Tokoro, K. Imoto, S. Ohkoshi and N. Mizuno, *Angew. Chem., Int. Ed.*, 2012, **51**, 1597; (*b*) Y. Kikukawa, K. Suzuki, M. Sugawa, T. Hirano, K. Kamata, K. Yamaguchi and N. Mizuno, *Angew. Chem., Int. Ed.*, 2012, **51**, 3686; (*c*) Y. Kikukawa, Y. Kuroda, K. Suzuki, M. Hibino, K. Yamaguchi and N. Mizuno, *Chem. Commun.*, 2013, **49**, 376; (*d*) K. Suzuki, R. Sato and N. Mizuno, *Chem. Sci.*, 2013, **4**, 596; (*e*) T. Hanaya, K. Suzuki, R. Sato, K. Yamaguchi and N. Mizuno, *Dalton Trans.*, 2017, **46**, 7384; (*f*) Y. Kuriyama, Y. Kikukawa, K. Suzuki, K. Yamaguchi and N. Mizuno, *Chem. –Eur. J.*, 2016, **22**, 3962.

(11) (*a*) K. Suzuki, R. Sato, T. Minato, M. Shinoe, K. Yamaguchi and N. Mizuno, *Dalton Trans.*, 2015*,* **44**, 14220; (*b*) K. Suzuki, R. Sato, T. Minato, K. Yamaguchi and N. Mizuno, *Inorg. Chem.*, 2016, **55**, 2023; (*c*) T. Minato, K. Suzuki, Y. Ohata, K. Yamaguchi and N. Mizuno, *Chem. Commun.*, 2017, **53**, 7533.

(12) (*a*) T. Minato, K. Suzuki, K. Yamaguchi and N. Mizuno, *Chem. –Eur. J.*, 2017, **23**, 14213; (*b*) J. Jeong, K. Suzuki, M. Hibino, K. Yamaguchi and N. Mizuno, *ChemistrySelect*, 2016, **1**, 5042.

(13) T. Minato, K. Suzuki, K. Yamaguchi and N. Mizuno, *Angew. Chem., Int. Ed.*, 2016, **55**, 9630.

(14) We have reported that acetimidate ligands, which were formed by hydration of acetonitrile, can coordinate on the vacant sites of lacunary POMs: (*a*) K. Suzuki, M. Shinoe, N. Mizuno, *Inorg. Chem.*, 2012, **51**, 11574; (*b*) J. Jeong, K. Suzuki, K. Yamaguchi, N. Mizuno, *New J. Chem.*, 2017, **41**, 13226.

(15) (*a*) C. R. Hamilton, M. R. Gau, R. A. Baglia, S. F. McWilliams and M. J. Zdilla, *J. Am. Chem. Soc.*, 2014, **136**, 17974; (*b*) T. Yamase, K. Fukaya, H. Nojiri and Y. Ohshima, *Inorg. Chem.*, 2006, **45**, 7698.

(16) G. D. Straganz, A. Glieder, L. Brecker, D. W. Ribbons and W. Steiner, *Biochem. J.*, 2003, **369**, 753.

(17) N. F. Chilton, R. P. Anderson, L. D. Turner, A. Soncini and K. S. Murray, *J. Comput. Chem.*, 2013, **34**, 1164.

(18) The *J* value of **Co2** could not be determined likely due to the large contribution of orbital angular momentum.

(19) (*a*) *CrystalClear* 1.3.6, Rigaku and Rigaku/MSC, The Woodlands, TX; (*b*) J. W. Pflugrath, *Acta Crystallogr.*, 1999, **D55**, 1718.

(20) Z. Otwinowski and W. Minor, Processing of X-ray Diffraction Data Collected in Oscillation Mode in *Methods in Enzymology*, C. W. Carter and Jr., R. M. Sweet, Eds., Macromolecular Crystallography, Part A, Academic press, New York, 1997, **276**, 307.

(21) *CrystalStructure* 3.8, Rigaku and Rigaku/MSC, TheWoodlands, TX.

(22) L. J. Farrugia, *J. Appl. Crystallogr.*, 1999, **32**, 837.

(23) (*a*) G. M. Sheldrick, SHELX97, *Programs for Crystal Structure Analysis*, Release 97-2, University of Göttingen, Göttingen, Germany, 1997; (*b*) G. M. Sheldrick, SHELX-2014, *Programs for Crystal Structure Analysis*, University of Göttingen, Göttingen, Germany, 2014.

(24) (*a*) I. D. Brown and Altermatt, *Acta Crystallogr.*, 1985, **B41**, 244; (*b*) N. E. Brese, and M. O'Keeffe, *Acta Crystallogr.*, 1991, **B47**, 192.

Table 1 Crystallographic data for Mn2, Co2, Ni2, Cu2, and Zn2

	Mn2	**Co2**	**Ni2**	**Cu2**	**Zn2**
Molecular formula	$C_{54}H_9Mn_2N_5O_{48}P_2W_{12}$	$C_{54}H_9Co_2N_5O_{48}P_2W_{12}$	$C_{54}H_9N_5Ni_2O_{48}P_2W_{12}$	$C_{54}H_9Cu_2N_5O_{48}P_2W_{12}$	$C_{54}H_9N_5O_{48}P_2W_{12}Zn_2$
Fw (g mol^{-1})	3873.57	3881.66	3881.08	3890.88	3894.48
Crystal system	orthorhombic	orthorhombic	orthorhombic	orthorhombic	orthorhombic
Space group	*C*2221	*C*2221	*C*2221	*C*2221	*C*2221
a (Å)	19.1135(2)	19.0803(2)	19.0988(2)	19.0981(2)	19.0793(2)
b (Å)	28.3342(3)	28.3426(3)	28.2884(4)	28.4851(3)	28.2796(3)
c (Å)	25.0357(3)	24.8868(3)	24.8669(3)	24.8371(3)	24.9170(3)
Volume (Å^3)	13558.5(3)	13458.4(3)	13435.0(3)	13511.7(3)	13444.1(3)
Z	4	4	4	4	4
Temp (K)	123(2)	123(2)	123(2)	123(2)	123(2)
ρ_{calcd} (g cm^{-3})	1.902	1.916	1.931	1.913	1.599
GOF	1.088	1.096	1.147	1.135	1.155
R_1 [$I > 2\sigma(I)$] [a]	0.0389	0.0528	0.0553	0.0477	0.0458
wR_2 [a]	0.1248	0.1625	0.1723	0.1536	0.1445

[a] $R_1 = \Sigma||F_o|-|F_c||/\Sigma|F_o|$, $wR_2 = \{\Sigma[w(F_o^2-F_c^2)]/\Sigma[w(F_o^2)^2]\}^{1/2}$.

Table 2 Selected bond lengths and angles for Mn2, Co2, Ni2, Cu2, and Zn2

	Mn2	**Co2**	**Ni2**	**Cu2**	**Zn2**
Bond length (Å)					
M1–O1	2.054	2.064	1.959	1.935	1.972
M1–O2	2.085	1.920	1.982	1.916	2.02
M1–O3	2.168	2.082	2.024	2.025	2.115
M1–O3*	2.207	2.153	2.074	2.031	2.114
M1–O101	2.083	2.129	1.981	2.105	1.963
M1···M1*	3.047	2.985	2.893	2.892	2.956
Bond angle (°)					
M1–O3–M1*	88.3	89.6	89.8	90.9	88.7

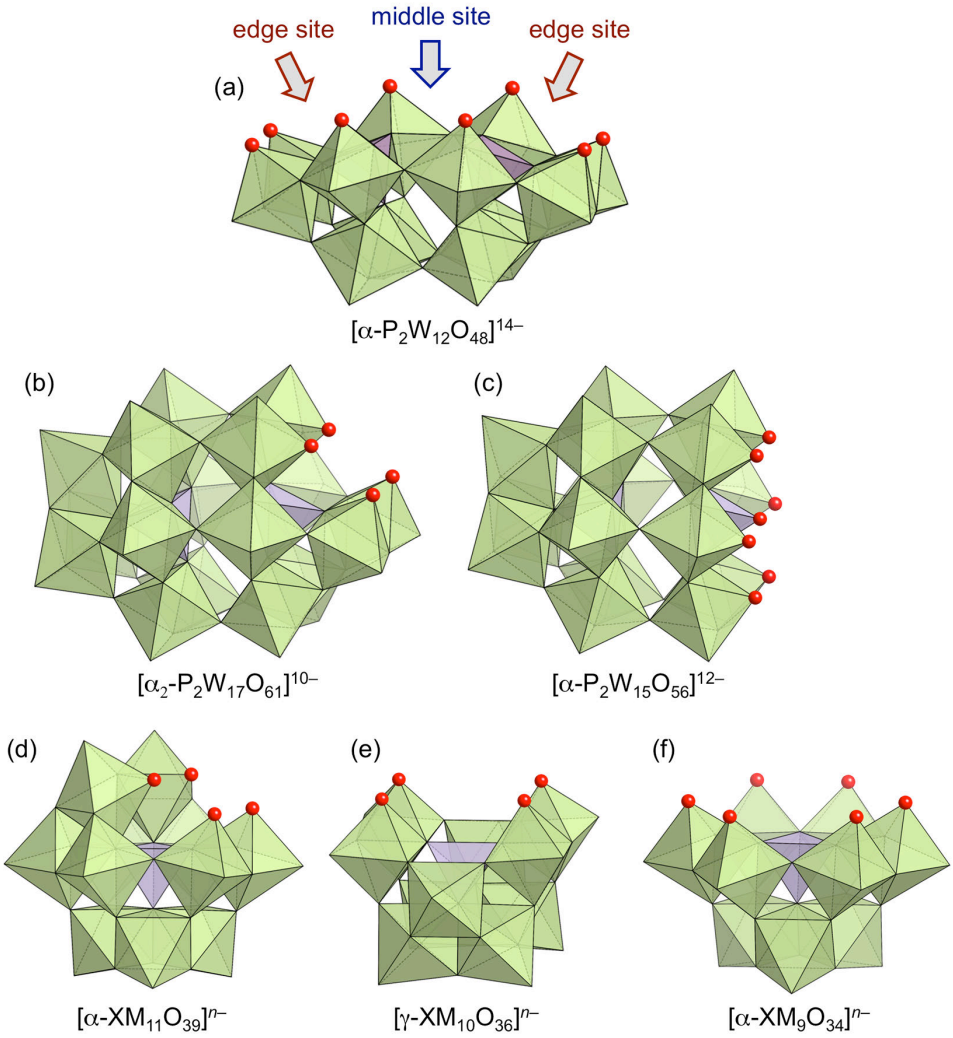

Fig. 1 Structures of lacunary POMs. (a) $[\alpha\text{-}P_2W_{12}O_{48}]^{14-}$, (b) $[\alpha_2\text{-}P_2W_{17}O_{61}]^{10-}$, (c) $[\alpha\text{-}P_2W_{15}O_{56}]^{12-}$, (d) $[\alpha\text{-}XM_{11}O_{39}]^{n-}$, (e) $[\gamma\text{-}XM_{10}O_{36}]^{n-}$, and (f) $[\alpha\text{-}XM_9O_{34}]^{n-}$.

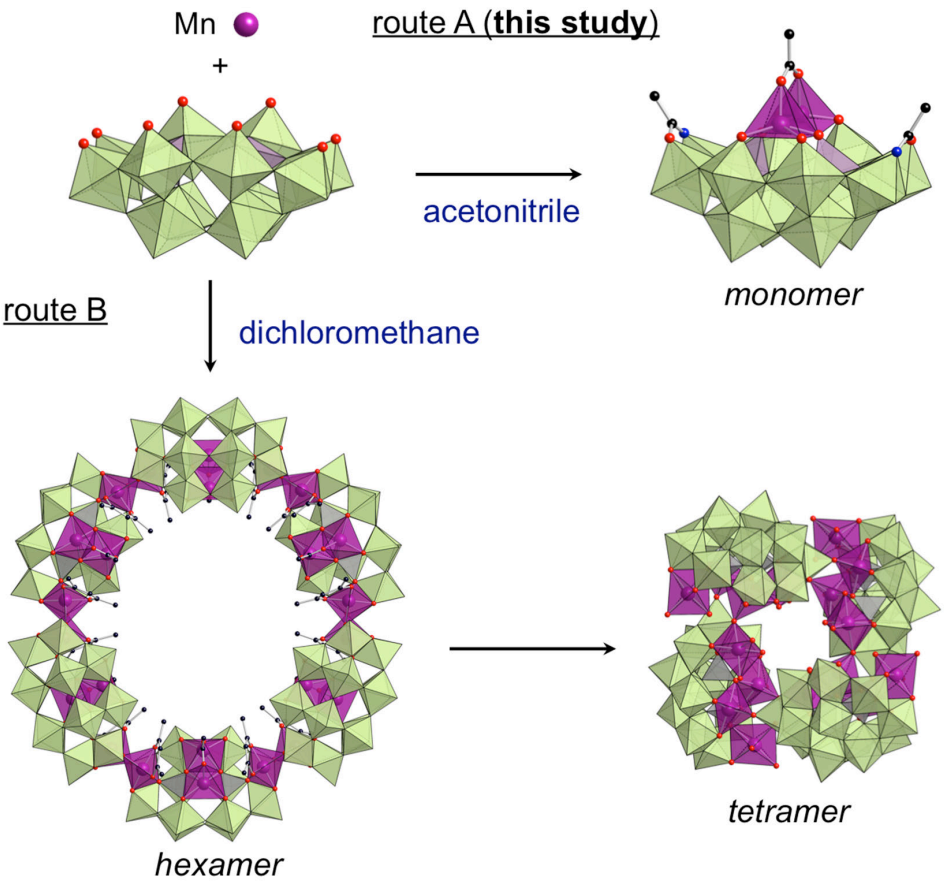

Fig. 2 The reaction between **I** and Mn in organic media. (route A) A monomer was selectively formed in acetonitrile by protecting the highly reactive sites using acetimidate ligands on the edge sites. (route B) A hexamer and a tetramer were formed in dichloromethane.[13]

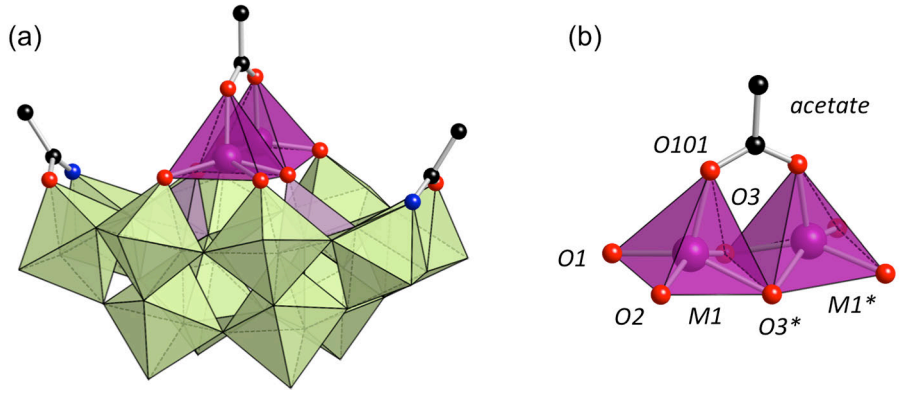

Fig. 3 Crystal structures of (a) anions and (b) dinuclear metal cores of **M2** (M = Mn, Co, Ni, Cu, Zn). Light green, gray, and purple polyhedra represent $\{WO_6\}$, $\{PO_4\}$, and $\{MO_5\}$, respectively. Black, blue, red, and purple spheres represent C, N, O, M atoms, respectively.

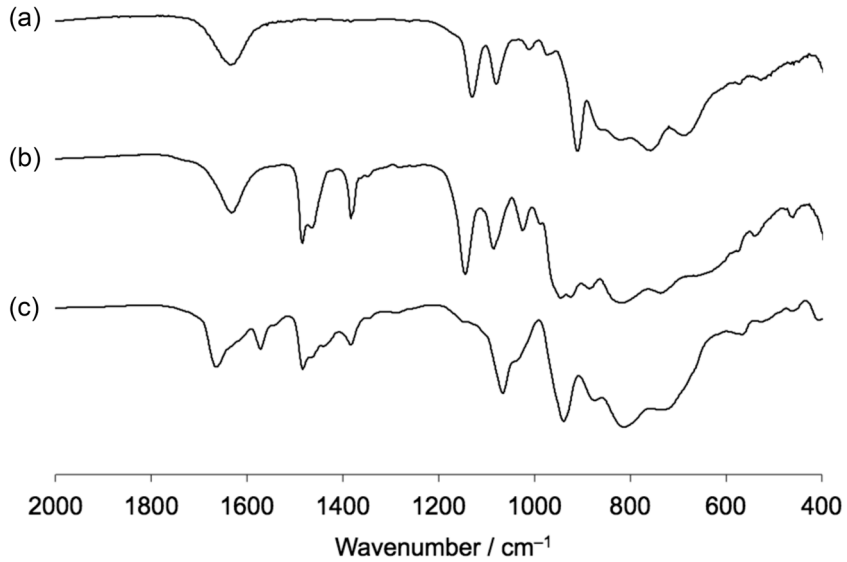

Fig. 4 IR spectra of (a) $K_{12}H_2[\alpha\text{-}P_2W_{12}O_{48}]\cdot 24H_2O$, (b) **I**, and (c) **Mn2**.

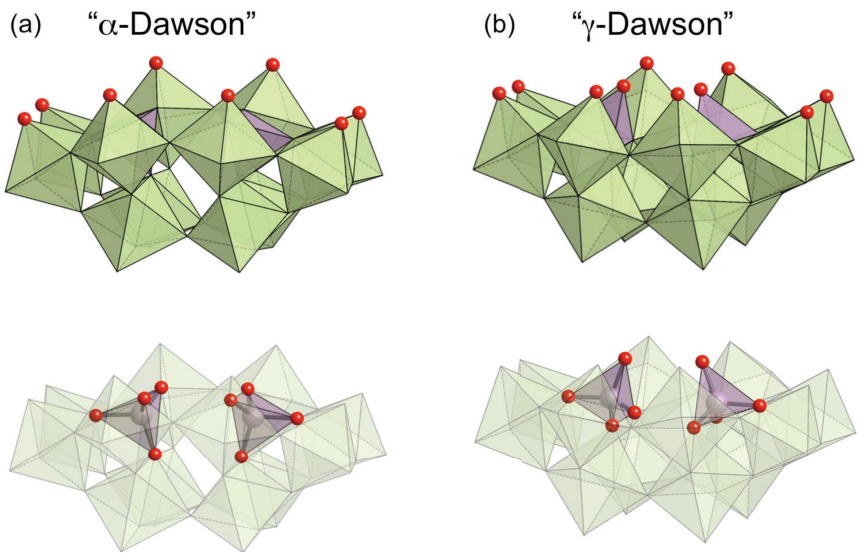

Fig. 5 Structures of hexavacant lacunary (a) α-Dawson-type POM $[\alpha\text{-}P_2W_{12}O_{48}]^{14-}$, and (b) **γ**-Dawson-type POM $[\gamma\text{-}P_2W_{12}O_{48}]^{14-}$. By flipping two $\{PO_4\}$ units, the hexavacant lacunary α-Dawson-type structure was transformed into γ-Dawson-type structure. Light green and gray polyhedra represent $\{WO_6\}$ and $\{PO_4\}$, respectively.

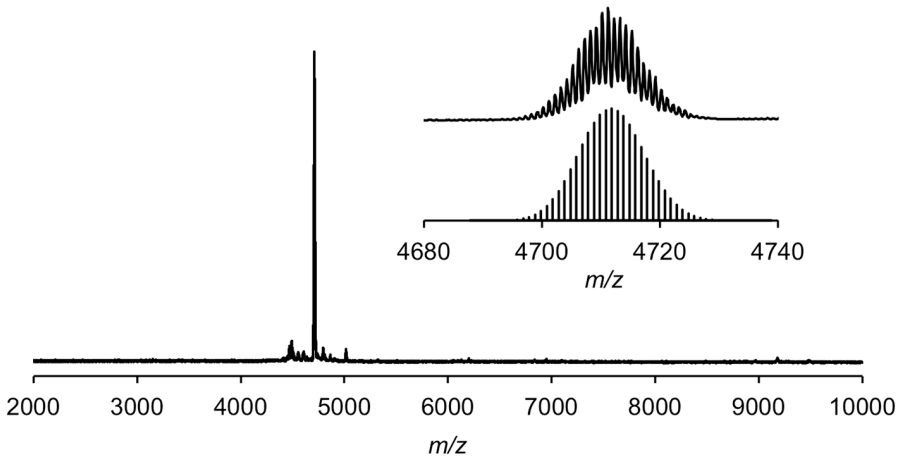

Fig. 6 Positive-ion CSI-mass spectrum of **Mn2** in acetonitrile. Inset: (top) spectrum in the *m/z* range of 4680–4740 and (bottom) the simulation pattern for $[TBA_6P_2W_{12}O_{44}Mn_2(OAc)(CH_3CONH)_2]^+$ (*m/z* 4711.8).

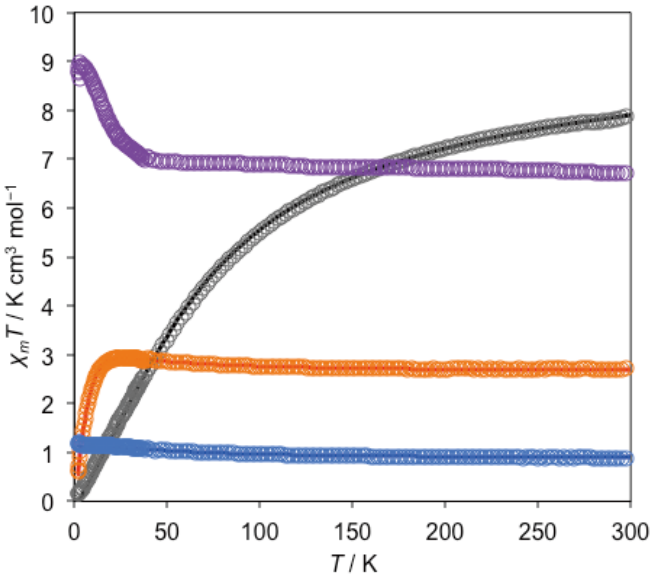

Fig. 7 Temperature dependence of χT for **M2** under an applied dc field of 0.1 T (gray, **Mn2**; purple, **Co2**; orange, **Ni**; blue, **Cu2**). Solid lines represent the best fits.

Table of Contents

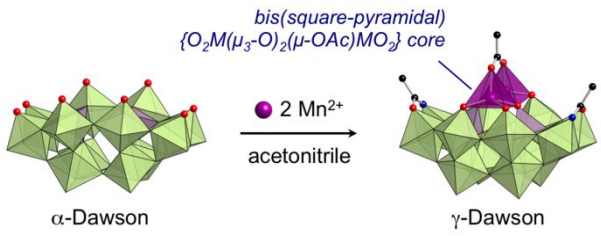

The reaction of a hexavacant lacunary α-Dawson-type phosphotungstate with divalent metal species in acetonitrile afforded a series of isostructural γ-Dawson-type structures supporting an edge-sharing bis(square-pyramidal) core.